RSC Advances

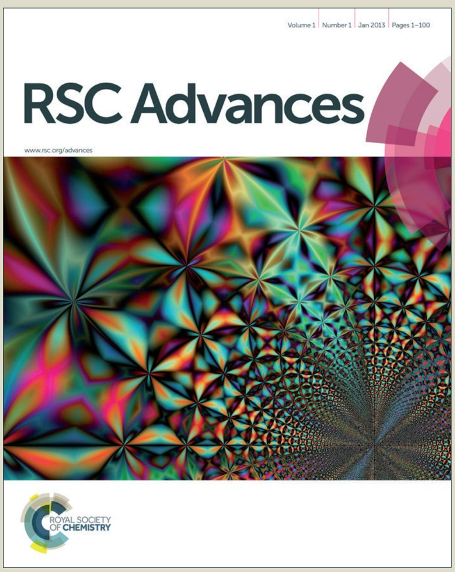

ROYAL SOCIETY OF CHEMISTRY

www.rsc.org/advances

Cite this: DOI: 10.1039/c0xx00000x

www.rsc.org/xxxxxx

ARTICLE TYPE

Core/shell structured Co/carbon nanotubes-graphene nanocomposites: synthesize and excellent electromagnetic absorption properties

Xiaosi Qi,*[a,b] Qi Hu,[a] Jianle Xu,[a] Ren Xie,[a] Yang Jiang,[a] Wei Zhong,*[a] Youwei Du[a]

Received (in XXX, XXX) Xth XXXXXXXXX 20XX, Accepted Xth XXXXXXXXX 20XX

DOI: 10.1039/b000000x

Abstract: Through the reduction process of Co_3O_4/reduced graphene oxide and acetylene, core/shell structured Co/carbon nanotubes-graphene nanocomposites were synthesized in large scale. Because of the special structure, high attenuation constant and good complementarities between magnetic loss material and dielectric loss material, the obtained Co/carbon nanotubes-graphene nanocomposites exhibit the very attractive microwave absorbing abilities. The optimal reflection loss (RL) can be up to -65.6 dB at 12.4 GHz with a matching thickness of 2.19 mm, and RL values below -20 dB can be obtained almost in the whole frequency range. Therefore, a simple approach was proposed to explore the high-performance microwave absorbing materials as well as expand the application field of graphene-based materials.

Keywords: Core/shell structured; Co/carbon nanotubes-graphene; Microwave absorption

1. Introduction

In recent decades, with the rapidly extensive application of wireless equipment, radar systems and local area networks, electromagnetic (EM) interference and EM compatibility have become serious problems, which not only limit the utilization of electronic devices and the development of modern military, but also are potentially harmful to humans [1-3]. In order to counteract these problems, microwave absorbing materials (MAMs), which can dissipate EM wave by converting it into thermal energy, have attracted more and more attention over the world [4-6]. It is well known that the microwave absorbing ability is mainly determined by the complex permittivity, the complex permeability and the EM impedance match of absorbers [7,8]. If the MAMs exhibit the optimal impedance matching conditions, the transmitted microwave can be dissipated by the dielectric loss and magnetic loss, and zero reflectivity of the incident microwave can be obtained. Therefore, it is difficult to meet these conditions over the sole dielectric loss materials or magnetic loss materials. In order to synthesize high performance of MAMs, various structures and categories of composites have been developed and investigated previously [9-13], and MAMs with light weight, thin thickness, good chemical stability, strong absorption ability and wide absorption frequency are still greatly desired.

Among these structures and materials, core/shell structured magnetic nanoparticles/carbon based composites, which possess low weight, strong chemical stability, good complementarities between the core substance and shell material, are promising candidates [14-16]. Because of its large surface area, high chemical and thermal stability, low mass density and outstanding electronic properties, graphene has evoked extensive interests in the past years [17-20]. The previously reported theoretic and experimental results indicated that the interfacial electronic interaction between metal particles and graphene could make graphene exhibits some novel physical properties [21-24]. Therefore, the microwave absorbing property investigation of magnetic metal particles/grapheme-based nanocomposites is of both fundamental and technological significance [25]. Herein, we report the synthesis of core/shell structured Co/carbon nanotubes-graphene nanocomposites and investigate their microwave absorption properties in details.

2. Experimental

2.1 Material preparation.

A certain amount of Co_3O_4/reduced graphene oxide (Co_3O_4/RGO) powder (purchased from XFNANO Materials Tech Co., Nanjing, China) was dispersed on a ceramic plate which was placed inside a quartz reaction tube. Subsequently, the tube furnace was heated from room temperature (RT) to 400 °C in Ar, and then a flow of acetylene (flow rate=30 mL/min) was introduced into the reaction tube at 400 °C for 2 h under atmospheric pressure. After cooling to RT in Ar, the final product was obtained.

2.2 Characterization of products.

The samples were examined on an X-ray powder diffractometer (XRD) at RT for phase identification using CuKα radiation (model D/Max-RA, Rigaku). Raman spectroscopic investigation was performed using a Jobin-Yvon Labram HR800 instrument with 514.5 nm Ar^+ laser excitation. The morphology investigations were examined using a transmission electron microscope (TEM) (model JEM-2000EX, operated at an accelerating voltage of 20 kV). The magnetic properties of samples were measured at 300 K using a Quantum Design MPMS SQUID magnetometer (Quantum Design MPMS-XL) equipped with a superconducting magnet capable of producing fields of up to 50 kOe. Surface properties of sample were studied by the Brunauer-Emmett-Teller (BET) methods via nitrogen adsorption and desorption measurements. For microwave measurement, 30 wt% of the as-prepared sample was mixed with paraffin and pressed into coaxial clapper in a dimension of outer diameter of 7.0 mm, inner diameter of 3.0 mm, respectively. The complex permittivity $(\varepsilon_r = \varepsilon_r' - j\varepsilon_r'')$ and complex permeability $(\mu_r = \mu_r' - j\mu_r'')$ of the composite were measured in frequency range of 2-18 GHz over an Agilent E8363B vector network analyzer. The attenuation constant (α) and reflection loss (RL) were calculated by the following equation [26,27]:

$$\alpha = \frac{\sqrt{2}\pi f}{c}\sqrt{(\mu''\varepsilon'' - \mu'\varepsilon') + \sqrt{(\mu''\varepsilon'' - \mu'\varepsilon')^2 + (\varepsilon'\mu'' + \varepsilon''\mu')^2}} \quad (1)$$

$$RL = 20\log\left|\frac{Z_{in} - 1}{Z_{in} + 1}\right| \quad (2)$$

$$Z_{in} = \sqrt{\frac{\mu_r}{\varepsilon_r}}\tanh\left(j\frac{2\pi fd\sqrt{\mu_r\varepsilon_r}}{c}\right) \quad (3)$$

where f is the frequency of the EM wave. d is the thickness of an absorber, c is the velocity of light and Z_{in} is the input impedance of absorber.

3. Results and discussion

3.1 Microstructures of Co_3O_4/RGO and Co/carbon nanotubes-graphene.

The morphologies of Co_3O_4/RGO and as-synthesized Co/carbon nanotubes-graphene were investigated by TEM. As shown in Figure 1a, the low magnification image indicates the Co_3O_4 nanoparticles (as indicated by the arrows) are inlaid in the layer structure graphene sheet. Moreover, the high magnification (as shown in Figure 1b) displays that the atom distance of Co_3O_4 is ca. 0.24 nm, which corresponds to the plane distance of (311). And the ultrathin structure of graphene can be observed clearly (as signed in Figure 1b) around the Co_3O_4 nanoparticles.

The morphology and structure of the obtained Co/carbon nanotubes-graphene were investigated by TEM observation. As shown in Figure 2a, the low TEM investigation indicates that different sizes of nanoparticles and carbon nanotubes are deposited on the surface of graphene. As indicated by the arrow in Figures 2b and c, one can find obviously the Co nanoparticles were tightly encapsulated by carbon nanotubes and layer structured graphene. The high resolution TEM image (as shown in Figure 2d) presents that the atom distance of Co is ca. 0.20 nm, which indicates the formation of crystalline Co nanoparticles. Therefore, core/shell structured Co/carbon nanotubes-graphene nanocomposites can be synthesized in large-scale by the method.

3.2 Crystal structure and magnetic property.

Figure 3a shows the XRD pattern of the obtained Co/carbon nanotubes-graphene. The diffraction peaks located at 41.8, 44.4, 47.3 and 51.6^o can be assigned to the phase of Co (JCPDS: 01-1254). Moreover, a diffraction peak at ca. 26.2^o can also be observed clearly, which can be assigned to the (002) crystal plane of hexagonal phase graphite (JCPDS: 75-1621). In order to identify the existence of graphene, the Raman spectra of Co_3O_4/RGO and Co/carbon nanotubes-graphene were obtained. As shown in Figure 3b, four peaks can be observed clearly over Co_3O_4/RGO and Co/carbon nanotubes-graphene. As indicated by the symbols in Figure 3b, these Raman peaks can be indexed to the D (disorder-induced), G (the tangential mode of graphite structure), 2D (intrinsic peak of graphene) and D+D´ band, respectively [28,29]. As we know that the ratio (I_D/I_G) is a measurement of disorder in structure. In the study, the obtained Co/carbon nanotubes-graphene presents a low I_D/I_G value (0.97) compared to that (1.00) of Co_3O_4/RGO, which may be related to the restoration of the sp^2 network as reported previously [30]. Moreover, compared to the previously reported graphene-based nanocomposites [31-33], the obtained Co/carbon nanotubes-graphene also shows a low I_D/I_G value, which indicates its high crystallinity. Generally, all the obtained results indicate that the as-synthesized sample is Co/carbon nanotubes-graphene. Based on the obtained results, the formation of core/shell Co/carbon nanotubes-graphene in our experimental process may be explained by the following reaction:

$$4C_2H_2 + 5Co_3O_4 \rightarrow 8CO_2 + 15Co + 4H_2O \quad (1)$$

$$C_2H_2 \xrightarrow{Co} 2C + H_2 \quad (2)$$

Through the aforementioned reactions, the formation of Co particles could be used as the catalyst for the growth of Co/carbon nanotubes-graphene effectively [34].

Figure 4 shows the magnetization curves at RT. One can find that the obtained Co/carbon nanotubes-graphene exhibits a typical ferromagnetic property. The saturation magnetization (M_s) and coercivity (H_c) of the sample are ca.19.7 emu g^{-1} and 488 Oe, respectively. The result also can confirm further the particles encapsulated in carbon nanotubes and graphene is ferromagnetic Co nanoparticles. Moreover, compared to the reported MnO_2@Fe-graphene and Fe/graphene [35,36], the obtained Co/carbon nanotubes-graphene displays a small M_s value.

3.3 Electromagnetic and microwave absorption properties.

Figure 5 gives the complex permittivity, complex permeability, dielectric loss and magnetic loss, and attenuation constant of Co/carbon nanotubes-graphene in the 2.0-18 GHz frequency range. As shown in Figure 5a, the ε' and ε'' values are in the range of 12.92-6.93 and 8.74-2.18, respectively. Moreover, as shown in Figure 5b, besides some fluctuations, the μ' values are close to 1.0 while the μ'' values are equal to 0. It is well known that the dielectric loss tangent ($\tan\delta_E = \varepsilon''/\varepsilon'$) and magnetic loss tangent ($\tan\delta_m = \mu''/\mu'$) are used to describe the dielectric loss and magnetic loss abilities. As shown in Figure 5c, one can find that the $\tan\delta_E$ values are much larger than those of $\tan\delta_m$ in the whole frequency range, indicating that the dielectric loss plays the main role in the EM absorption. Besides, Compared to those graphene-based nanocomposites reported elsewhere [37,38], the obtained Co/carbon nanotubes-graphene exhibits good complementarities between the dielectric loss and magnetic loss, which favours a strong EM attenuation. These excellent complementarities should be related to its core/shell structure [39]. In order to understand the microwave absorption properties of Co/carbon nanotubes-graphene well, as shown in Figure 5d, the values of attenuation constant α [as expressed in equation

(1)] in the whole frequency range were obtained. The obtained α values are in the range of 43-197, which is much higher than the previously reported MnO_2@Fe-graphene nanocomposites [33]. It is noted that the attenuation constant α represents integral attenuation ability. In other words, the higher α values may indicate the excellent attenuation or microwave absorption.

According to Equations. (2) and (3), the RL values of the as-synthesized Co/carbon nanotubes-graphene nanocomposites were obtained from the measured complex permeability and permittivity at the given frequency, and the results are shown in Figure 6. Figure 6a show the color map of RL values. It is obvious that the minimum RL moves toward to the lower frequency region with an increasing thickness, and a minimum RL value of -65.6 dB was observed at 12.4 GHz with a matching thickness of 2.19 mm, which can also be confirmed by the typical result as shown in Figure 6b. Moreover, RL values below -20 dB (99% of EM wave attenuation) can be obtained almost in the whole frequency range. Figure 6c shows the typical RL values obtained with the matching thicknesses of 1.9 mm. One can find that the optimum RL value of -43.8 dB can be observed at 13.8 GHz. Generally speaking, compared to those representative graphene nanocomposites (as shown in Table 1), the obtained Co/carbon nanotubes-graphene nanocomposites exhibit an excellent microwave absorbing ability.

In order to understand the excellent microwave absorption mechanism, the previously reported models such as zero reflection and geometrical effect were used to interpret the enhanced EM absorption properties [45,46]. As we well known that, in terms of EM wave theory, $\mu_r = \varepsilon_r$ should be satisfied for zero reflection. However, as shown in Figures 5a and b, the obtained value of ε_r is much higher those of μ_r. And the geometrical effect is strongly dependent on the equation (4):

$$t = \frac{n\lambda_m}{4} \ (n = 1,3,5,\cdots) \qquad (4)$$

where $\lambda_m = \frac{c}{f_m\sqrt{|\mu_r||\varepsilon_r|}}$. According to the minimum data of RL, the matching frequency and the corresponding μ_r and ε_r, Substituting these values into equation (4), the obtained thickness is ca. 1.98 mm, which is not closed to the obtained matching thickness of 2.19 mm. Therefore, one can find easily that the zero reflection and geometrical effects cannot account for the excellent EM absorption properties of Co/carbon nanotubes-graphene. Based on the obtained results and the recent mechanisms reported by Ren et. al and Zhang et al. [47-50], we also think that the excellent microwave absorption properties of Co/carbon nanotubes-graphene nanocomposites should be related to their special structure and synergetic effect. First, according to the Cole-Cole dispersion laws, the Debye relaxation process can be reflected by the plot of $\varepsilon' - \varepsilon''$, and the enhanced Debye relaxation process induced by the interfaces can improve the EM absorption properties. As shown in Figure 7a, one can find that the Co/carbon nanotubes-graphene nanocomposites have much more semicircles than the reported graphene-based nanocomposites elsewhere [49], which indicates the interface polarization plays an important role in the excellent microwave absorption properties. Second, the Co nanoparticles grown on the graphene sheets can decrease the resistance (R) of the absorbers. According to $\varepsilon'' \propto \sigma/2\pi\varepsilon_0 f$, the decreasing of R will lead to the increasing of dielectric loss. Third, as shown in Figure 7b, the BET surface area of the Co/carbon nanotubes-graphene is 71.4 m^2/g, which favours the formation of much more dipoles. And the dipole polarizations will contribute to the enhanced EM absorption properties [51]. In addition, as shown in Figure 5c, Compared to the previously reported graphene-based nanocomposites [33,37,38,47-50], much higher values of α, and much better complementarities between dielectric loss and magnetic loss can be observed over the obtaiend Co/carbon nanotubes-graphene nanocomposites.

4. Conclusions

In the study, through the reduction process of Co_3O_4/RGO and acetylene, core/shell structured Co/carbon nanotubes-graphene nanocomposites were synthesized in large scale. Because of the special structure, high α values and good complementarities between magnetic loss and dielectric loss, the obtained Co/carbon nanotubes-graphene nanocomposites exhibit excellent microwave absorbing properties. The minimum RL of ca. -65.6 dB at 12.4 GHz with a matching thickness of 2.19 mm was observed, and RL values below -20 dB can be obtained almost in the whole frequency range. The obtained results indicate that the obtained Co/carbon nanotubes-graphene nanocomposites may be a promising light-weight material effective for microwave absorption.

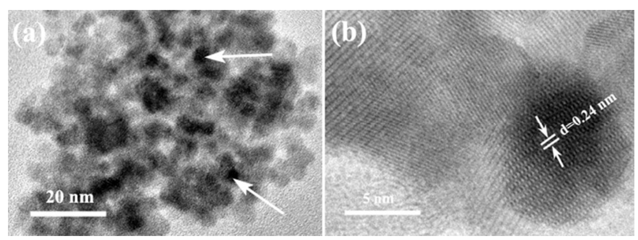

Figure 1. (a) Low, and (b) high resolution TEM images of Co_3O_4/RGO.

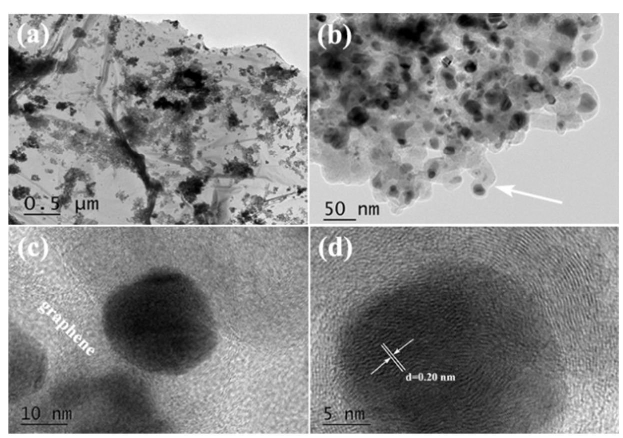

Figure 2. (a) Low, and (b-d) high resolution TEM images of Co/carbon nanotubes-graphene.

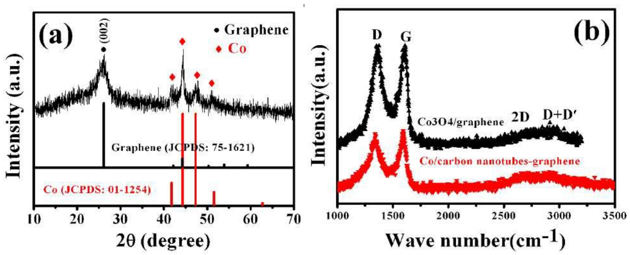

Figure 3. (a) XRD pattern of Co/carbon nanotubes-graphene, and (b) Raman spectra of Co_3O_4/RGO and Co/carbon nanotubes-graphene.

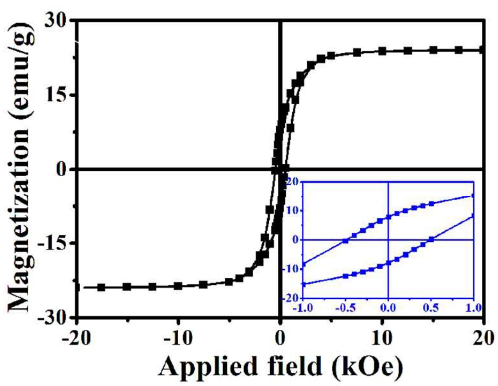

Figure 4. The magnetic hysteresis loop for Co/carbon nanotubes-graphene at RT (inset is the enlarged part close to the origin).

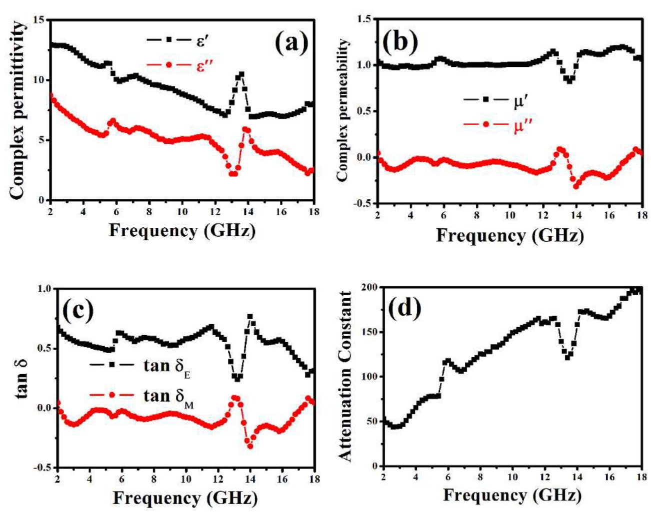

Figure 5. (a) Complex permittivity, (b) complex permeability, (c) loss tangent, and (d) attenuation constant versus frequency of Co/carbon nanotubes-graphene.

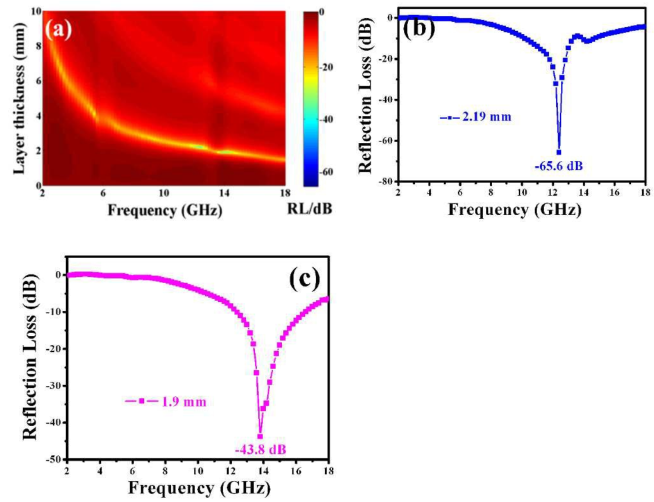

Figure 6. (a) Two-dimensional representation RL values, and (b,c) the typical RL values obtained with the thicknesses of 2.19 and1.9 mm as a function of frequency for Co/carbon nanotubes-graphene.

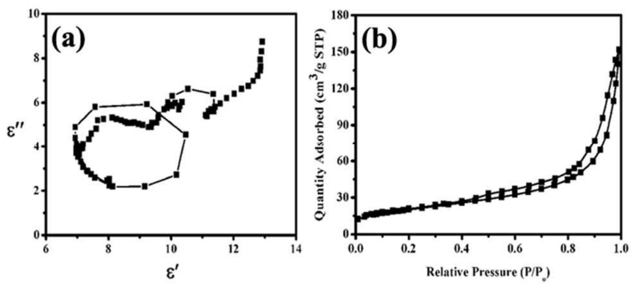

Figure 7. (a) Core-core semicircles, and (b) N_2 adsorption and desorption isotherms of Co/carbon nanotubes-graphene.

Table 1. Electromagnetic absorption properties of graphene-based composites reported in recent representative papers.

MAMs (Absorbent content)	Optimum RL (dB)	Optimum thickness (mm)	Frequency range (GHz) (RL<-20 dB)	Reference
$FeNi_3$@ SiO_2-RGO[a] (10 wt%)	-49.4	3.8	5.0-11.0	31
MnO_2@Fe-G[b] (50 wt%)	-17.5	1.5		35
Fe@G (40 wt%)	-45	3.0	4.0-18.0	36
G-Fe_3O_4 (20 t%)	-40.3	5.0	4.0-13.0	37
G-Ni (30 wt%)	-42	2.0	12.0-18.0	38
Fe_2O_3@G (45 wt%)	-59.6	2.5		40

G@$CoFe_2O_4$@SiO_2@TiO_2 (-)	-62.8	4.9	4.5-18.0	41
$NiFe_2O_4$@RGO (-)	-47.3	2.5	7.0-15.0	42
$NiFe_2O_4$@G (60 wt%)	-29.2	2.0	5.7-17.5	43
G/hexaferrite (20 wt%)	-58	3.0	8.0-12.5	44
Co/carbon nanotubes-G (30 wt%)	-65.6	2.19	2.5-18.0	this work

[a]$FeNi_3$@SiO_2-reduced graphene oxide

[b]MnO_2@Fe-graphene

Acknowledgments

This work was supported by the International Cooperation Project of Guizhou Province (2012-7002), the Excellent Talents of Guizhou Province (2014-239), the National Science Foundation of Guizhou province (2014-2059), the Postdoctoral Science Foundation of China (2015M570427), the Science and Technology Innovation Team of Guizhou province (2015-4017), the National Science Foundation of China (Grant Nos. 11364005 and 11174132), and the Foundation of the National Key Project for Basic Research (2012CB932304 and 2011CB922102) for financial support.

Notes and references

[a]*Physics Department, Guizhou University, Guiyang 550025, People's Republic of China*
[b]*Nanjing National Laboratory of Microstructures and Jiangsu Provincial Laboratory for NanoTechnology, Nanjing University, Nanjing 210093, People's Republic of China*
Fax: +86-25-83595535; Tel: +86-25-83621200;
E-mail:xsqi@gzu.edu.cn, wzhong@nju.edu.cn

1 M. S. Cao, J. Yang, W. L. Song, D. Qi Zhang, B. Wen, H. B. Jin, Z. L. Hou and J. Yuan, *ACS Appl. Mater. Inter.*, 2012, **4**, 6949-6956.
2 W. L. Song, M. S. Cao, L. Z. Fan, M. M. Lu, Y. Li, C. Y. Wang and H. F. Ju, *Carbon*, 2014, **77**, 130-142.
3 Y. Chen, X. Y. Liu, X. Y. Mao, Q. X. Zhuang, Z. Xie and Z. W. Han, *Nanoscale*, 2014, **6**, 6440–6447.
4 J. R. Liu, M. Itoh and K. Machida, *Appl. Phys. Lett.*, 2003, **83**, 4017–4019.
5 C. R. Che, M. L. Peng, F. X. Duan, Q. Chen and L. X. Liang, *Adv. Mater.*, 2004, **16**, 401–405.
6 M. Fu, Q. Z. Jiao, Y. Zhao and H. S. Li, *J. Mater. Chem. A*, 2014, **2**, 735–744.
7 R. L. Ji, C. B. Cao, Z. Chen, H. Z. Zhai and J. Bai, *J. Mater. Chem. C*, 2014, **2**, 5944–5953.
8 Y. Liu, X. X. Liu, R. Li, W. Wen and X. J. Wang, *RSC Adv.*, 2015, **5**, 8713–8720.
9 P. M. Sudeep, S. Vinayasree, P. Mohanan, P. M. Ajayan, T. N. Narayanan and M. R. Anantharaman, *Appl. Phys. Lett.*, 2015, **106**, 221603.
10 P. Saini, M. Arora, G. Gupta, B. K. Gupta, V. N. Singh and V. Choudhary, *Nanoscale*, 2013, **5**, 4330–4336.
11 P. Saini, V. Choudhary, N. Vijayan and R. K. Kotnala, *J. Phys. Chem. C*, 2012, **116**, 13403–13412.
12 H. B. Zhang, Q. Yan, W. G. Zheng, Z. He and Z. Z. Yu, *ACS Appl. Mater. Inter.*, 2011, **3**, 918–924.
13 Y. L. Ren, C. L. Zhu, S. Zhang, C. Y. Li, Y. J. Chen, P. Gao, P. P. Yang and Q. Y. Ouyang, *Nanoscale*, 2013, **5**, 12296–12303.
14 J. Liu, J. Cheng, R. Che, J. Xu, M. Liu and Z. Liu, *J. Phys. Chem. C*, 2013, **117**, 489–495.
15 J. Y. Chen, G. Xiao, S. T. Wang, Y. Q. Ouyang, H. L. Qi and Y. Ma, *J. Phys. Chem. C*, 2011, **115**, 13603–13608.
16 G. X. Liu, Y. D. Geng, H. Meng, J. P. Shang and D. Z. Zhang, *Appl. Phys. Lett.*, 2008, **92**, 173117.
17 A. K. Geim and K. S. Novoselov, *Nat. Mater.*, 2007, **6**, 183–191
18 A. K. Geim, *Science*, 2009, **324**, 1530–1534.
19 G. Z. Magda, X. Z. Jin, I. Hagymasi, P. Vancso, Z. Osvath, P . Nemes-Incze, C. Y. Hwang, L. P. Biro and L. Tapaszto, *Nature*, 2014, **514**, 608-611.
20 S. Garaj, W. Hubbard, A. Reina, J. Kong, D. Branton and J. A. Golovchenko, *Nature*, 2010, **467**, 190-193
21 G. Giovannetti, P. A. Khomyakov, G. Brocks, V. M. Karpan, J. van den Brink and P. J. Kelly, *Phys. Rev. Lett.*, 2008, **101**, 026803.
22 P. A. Khomyakov, G. Giovannetti, P. C. Rusu, G. Brocks, J. van den Brink and P. J. Kelly. *Phys. Rev. B*, 2009, **79**, 195425.
23 W. Li, Y. H. He, L. Wang, G. H. Ding, Z. Q. Zhang, R. W. Lortz, P. Sheng and N. Wang. *Phys. Rev. B*, 2011, **84**, 045431.
24 D. S. Yu and M. Fonin, *New J. Phys.*, 2010, **12**, 125004.
25 C. Wang, X. J. Han, P. Xu, X. L. Zhang, Y. C. Du, S. R. Hu, J. Y. Wang and X. H. Wang, *Appl. Phys. Lett.*, 2011, **98**, 072906.
26 E. Michielssen, J. M. Sager, S. Ranjithan and R. Mittra, *Microwave Theory Tech.*, 1993, **41**, 1024-1031.
27 A. N. Yusoff, M. H. Abdullah, S. H. Ahmad, S. F. Jusoh, A. A. Manso and S. A. A. Hamid, *J. Appl. Phys.*, 2002, **92**, 876-882.
28 R. H. Rickman and P. R. Dunstan, *J. Raman Spectrosc.*, 2014, **45**, 15-21.
29 E. H. Martins Ferreira, M. V. O. Moutinho, F. Stavale , M. M. Lucchese, R. B. Capaz, C. A. Achete and A. Jorio, *Phys. Rev. B*, 2010, **82**, 125429.
30 P. B. Liu, Y. Huang and X. Sun, *ACS Appl. Mater. Inter.*, 2013, **5**, 12355-12360.
31 X. Ding, Y. Huang and M. Zong, *Mater. Lett.*, 2015, **157**, 285-289.
32 X. F. Song, M. J. Wang, D. P. Wei, D. Liu, H. F. Shi, C. G. Hu, L. Fang, W. Zhang and C. L. Du, *J. Alloy Compd.*, 2015, **651**, 230-236.
33 H. L. Xu, H. Bai and R. B. Yang, *J. Appl. Phys.*, 2012, **111**, 07A522.
34 S. Esconjauregui, C.M. Whelan and K. Maex, *Carbon*, 2009, **47**, 659-669.
35 H. L. Lv, G. B. Ji, X. H. Liang, H. Q. Zhang and Y. W. Du, *J. Mater. Chem. C*, 2015, **3**, 5056-5064.
36 X. C. Zhao, Z. M. Zhang, L. Y. Wang, K. Xi, Q. Q. Cao, D. H. Wang, Y. Yang and Y. W. Du, *Sci. Rep.*, 2013, **3**, 3421.
37 T. S. Wang, Z. H. Liu, M. M. Lu, B. Wen, Q. Y. Ouyang, Y. J. Chen, C. L. Zhu, P. Gao, C. Y. Li, M. S. Cao and L. H. Qi, *J. Appl. Phys.*, 2013, **113**, 024314.
38 Z. T. Zhu, X. Sun, G. X. Li, H. R. Xue, H. Guo, X. L. Fan, X. C. Pan and J. P. He, *J. Magn. Magn. Mater.*, 2015, **377**, 95-103.
39 X. S. Qi, W. Zhong, C. Y. Deng, C. T. Au and Y. W. Du, *Mater. Lett.*, 2013, **107**, 374-377.
40 L. Kong, X. W. Yin, Y. J. Zhang, X. Y. Yuan, Q. Li, F. Ye, L. F. Cheng and L. T. Zhang, *J. Phys. Chem. C*, 2013, **117**, 19701–19711.
41 X. Zhang, Y. Huang, X. F. Chen, C. Li and J. J. Chen, *Mater. Lett.*, 2015, **158**, 380-383.
42 P. B. Liu, Y. Huang and X. Sun, *Mater. Lett.*, 2013, **112**, 117-120.
43 M. Fu, Q. Z. Jiao and Y. Zhao, *J. Mater. Chem. A*, 2013, **1**, 5577-5586.
44 Z. Durmus, A. Durmus and H. Kavas, *J. Mater. Sci.*, 2015, **50**, 1201-1213.
45 J. W. Liu, R. C. Che, H. J. Chen, F. Zhang, F. Xia, Q. S. Wu and M. Wang, *Small*, 2012, **8**, 1214-1221.
46 A. N. Yusoff, M. H. Abdullah, S. H. Ahmad, S. F. Jusoh, A. A. Mansor and S. A. A. Hamid, *J. Appl. Phys.*, 2002, **92**, 876-882.

47 Y. L. Ren, C. L. Zhu, L. H. Qi, H. Gao and Y. J. Chen, *RSC Adv.*, 2014, **4**, 21510-21516.
48 Y. L. Ren, C. L. Zhu, S. Zhang, C. Y. Li, Y. J. Chen, P. Gao, P. P. Yang and Q. Y. Ouyang, *Nanoscale*, 2013, **5**, 12296-12303.
49 Y. L. Ren, H. Y. Wu, M. M. Lu, Y. J. Chen, C. L. Zhu, L, P. Gao, M. S. Cao, C. Y. Li and Q. Y. Ouyang, *ACS Appl. Mater. Interfaces*, 2012, **4**, 6436-6442.
50 H. M. Zhang, C. L. Zhu, Y. J. Chen and H. Gao, ChemPhysChem., 2014, 15, 2261-2266.
51 T. S. Wang, Z. H. Liu, M. M. Lu, B. Wen, Q. Y. Ouyang, Y. J. Chen, C. L. Zhu, P. Gao, C. Y. Li, M. S. Cao and L. H. Qi, *J. Appl. Phys.*, 2013, **113**, 024314.

Core/shell structured Co/carbon nanotubes-graphene nanocomposites: synthesize and excellent electromagnetic absorption properties Xiaosi Qi, Qi Hu, Jianle Xu, Ren Xie, Yang Jiang, Wei Zhong, Youwei Du	In the article, we report the synthesis of core/shell structured Co/carbon nanotubes-graphene nanocomposites. The obtained Co/carbon nanotubes-graphene nanocomposites exhibit the very attractive microwave absorbing abilities. The optimal reflection loss can be up to -65.6 dB at 12.4 GHz with a matching thickness of 2.19 mm, and RL values below -20 dB can be obtained almost in the whole frequency range.